GRANT
IN-35-CR
418

Contract No. NAG5-859

Semi-Annual Report

The Absolute Radiometric Calibration of the Advanced Very High Resolution Radiometer

P. N. Slater, P. M. Teillet and Y. Ding

Optical Sciences Center
The University of Arizona
Tucson, Arizona 84721

Goddard Space Flight Center
Greenbelt, Maryland 20771

October 1988

Summary

During the last six months of grant NAG5-859 there have been several additional calibration campaigns involving the NOAA-9 AVHRR. This report describes work conducted at Rogers (Dry) Lake, California.

Those involved in the measurements and data reduction were P. M. Teillet, Y. Ding, D. I. Gellman, R. D. Jackson, M. S. Moran and P. N. Slater.

1. Introduction

An increasing number of remote sensing investigations require radiometrically calibrated imagery from NOAA Advanced Very High Resolution Radiometer (AVHRR) sensors. Although a prelaunch calibration is done for these sensors, there is no capability for monitoring any changes in the in-flight absolute calibration for the visible and near infrared spectral channels. Hence, the possibility of using the reflectance-based method developed at White Sands for in-orbit calibration of Landsat Thematic Mapper (TM) and SPOT Haute Resolution Visible (HRV) data to calibrate the AVHRR sensor has been under investigation. Three different approaches have been considered.

(i) Method 1: Ground and atmospheric measurements **and reference** to another calibrated satellite sensor.

Ground reflectance measurements can be made over terrain areas corresponding to numerous Landsat TM pixels, but such measurements become impractical for the calibration of the AVHRR image data with pixel dimensions of 1.1 km by 1.1 km or greater. An alternative is to acquire AVHRR imagery of White Sands on the same day that a TM calibration has been carried out on the basis of ground reflectance factor and atmospheric measurements at Chuck Site in the alkali-flat region of White Sands. The methodology then takes advantage of the accurate calibration results for TM bands 3 and 4 to effect a calibration of AVHRR channels 1 and 2.

More specifically, a relatively uniform area corresponding to several AVHRR pixels is selected in the alkali-flat region and average digital counts are extracted for these AVHRR pixels and for pixels from the matching area in the TM imagery. With the help of radiative transfer

computations and bidirectional reflectance data for the gypsum surface at White Sands, radiance at the entrance aperture of the AVHRR sensor is predicted. The analysis takes into account differences in spectral response, sun angle, and viewing geometry between the TM and AVHRR data acquisitions.

(ii) Method 2: Ground and atmospheric measurements with no reference to another sensor.

The second approach is somewhat analogous to the original reflectance-based approach used at White Sands to calibrate the TM or HRV sensors (Slater et al., 1987a). It is based on detailed ground and atmospheric measurements near the time of AVHRR overpass, but it necessarily assumes the reflectance values to be representative of the whole pixel since these ground measurements can only encompass a portion of one AVHRR pixel. The availability of aircraft data can assist in the selection of an appropriately uniform area for this purpose. Although this method is not likely to be as accurate as the first, it has the distinct advantage of not requiring nearly coincident data acquisition from two different sensors.

(iii) Method 3: No ground and atmospheric measurements but reference to another satellite sensor.

As with the first method, this approach achieves a calibration of the first two AVHRR channels by reference to another satellite sensor such as the TM on the same day. However, it differs significantly in that no ground and atmospheric measurements on the overpass day are needed. Instead, a standard data set of atmospheric conditions is used to approximate the actual atmosphere and historical bidirectional reflectance data are used to adjust for differences in illumination and viewing geometries. The same atmospheric parameters are adopted to estimate surface reflectance from the TM imagery and then to predict radiance at the AVHRR sensor from that surface reflectance (suitably adjusted for bidirectional effects and spectral bandpass differences). Because of this two-way use of the atmospheric model, errors introduced in one direction will be compensated to some extent in the reverse direction so that reasonable calibration results can be obtained if the procedure is not overly sensitive to the choice of atmospheric model.

If it proves to be viable, this approach will be a valuable one because it will facilitate in-orbit sensor calibration without the complexity and expense of field measurements.

The purpose of this report is to describe an investigation on the use of Method 2 (Figure 1.1) to calibrate NOAA-9 AVHRR channels 1 and 2 with the help of ground and atmospheric measurements at Rogers (dry) Lake, Edwards Air Force Base (EAFB) in the Mojave desert of California. NOAA-9 has an ascending orbit in the daytime, with an equatorial crossing near three o'clock in the afternoon, local time. The first two AVHRR channels are rather broad, spanning the spectral regions from 570 to 700 nanometers and 714 to 983 nanometers. Three NOAA-9 AVHRR images were studied: October 14, 1986, May 4, 1987, and May 5, 1987.

The ground measurement area is located at the North end of EAFB on the dry lakebed of Rogers Lake. Compared to White Sands, New Mexico, the dry mud surface is flatter, more uniform spatially, and spectrally fairly flat. The ground does have a network of cracks everywhere, but on a scale that is not important for the measurements involved. More troublesome is the strong non-lambertian character of the surface, which can exhibit strong specular reflection when off-nadir observations are made in the direction toward the sun. Another disadvantage of the site is the need for constant radio contact with the air-traffic control in case the area has to be cleared rapidly. Nevertheless, the site lends itself well to the in-flight calibration of sensors such as the Airborne Imaging Spectrometer (AIS) and the Advanced Visible and Infrared Imaging Spectrometer (AVIRIS), as well as the in-orbit calibration of satellite sensors.

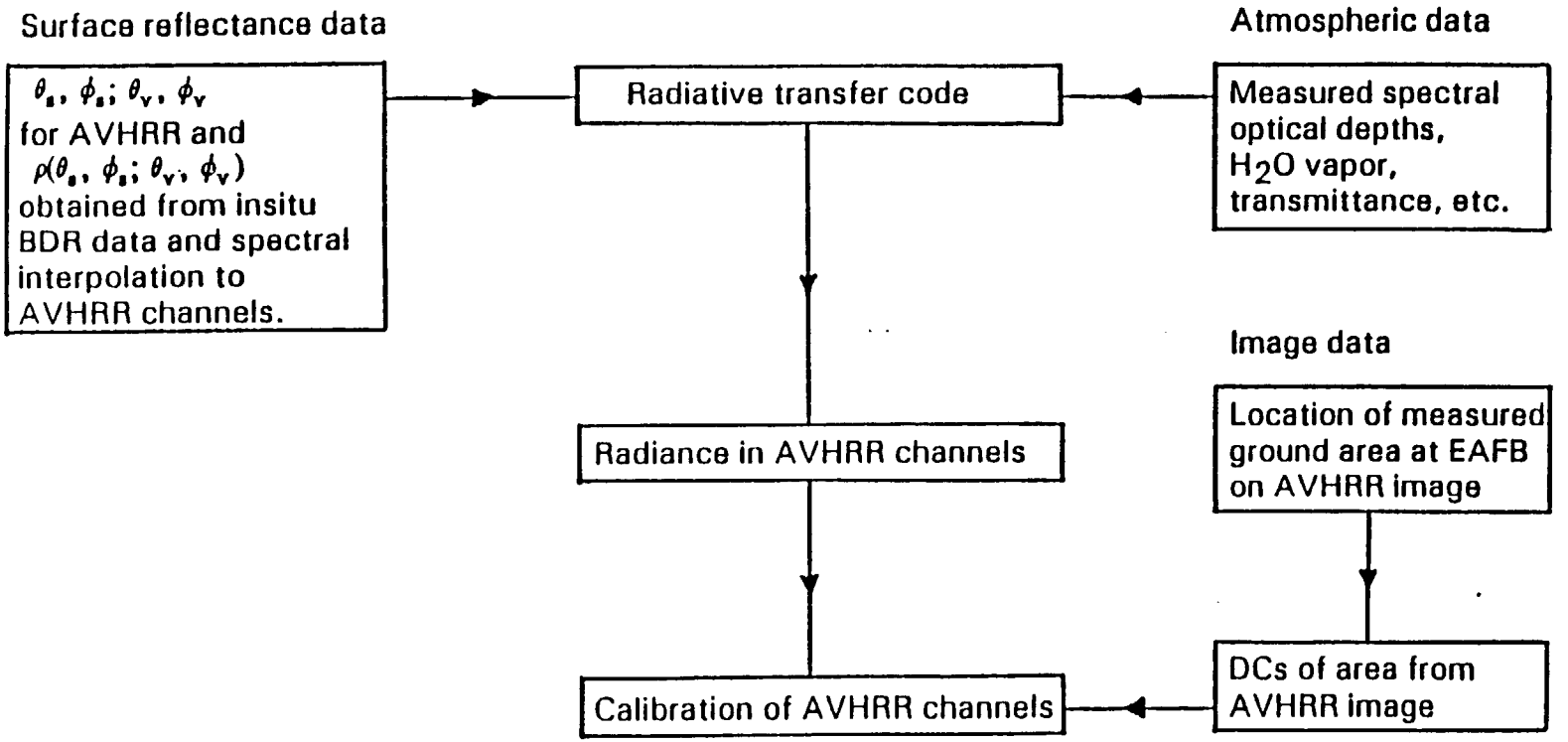

Figure 1.1 "Method 2" calibration approach: ground and atmospheric measurements without reference to another sensor.

2. Atmospheric Data Reduction

The Method 2 calibration approach discussed in this report relies on atmospheric measurements made at the site on the day of an overpass. In particular, Rayleigh, aerosol and ozone optical depth values are required by the radiative transfer code used to predict radiance at the entrance aperture of the satellite sensor from the terrain reflectance measured on the ground. The Rayleigh optical depth was determined from a knowledge of the barometric pressure and wavelength. The total optical depths were determined from the slopes of Langley plots in which the log voltages from solar radiometers were plotted against air masses. In spectral regions unaffected by absorption, the Mie (aerosol) optical depth at any wavelength was determined by subtracting the Rayleigh from the total optical depth at that wavelength. An optical depth versus wavelength curve was fitted through the points that spanned the absorption region due to ozone. The differences between the values on this curve at a given wavelength and the total minus Rayleigh value at the same wavelength gave the ozone optical depth at that wavelength. A Junge radial size distribution (Junge, 1963) was assumed for the aerosols. The Junge parameter, ν, is given by

$$\frac{dN}{dr} = cr^{-(\nu+1)},$$

where N is the number of particles, r is their radius, and c is a constant. The value of ν, needed to find the aerosol phase function, was determined from the slope of the log (Mie optical depth) versus log (wavelength) curve.

Solar radiometer measurements were made next to the dry lakebed at EAFB on October 14, 1986, May 4, 1987, and May 5, 1987. More specifically, on October 14, data were collected throughout the morning in order to generate a Langley plot. On May 4, it was only possible to obtain some instantaneous extinction data within a few minutes of the NOAA-9 overpass. The next day, May 5, data were collected from early morning to mid-afternoon, after the NOAA-9 overpass. In all cases, a manually operated solar radiometer designed by Dr. John A. Reagan of the University of Arizona was used. The Reagan instrument uses a single spectral filter wheel and a single silicon detector, obtaining readings in nine spectral bands from 0.400 to 1.03 micrometers.

Optical depth values obtained from the atmospheric data reduction involving nine wavelengths were then interpolated at the wavelengths used later in the analysis of AVHRR channels 1 and 2. Since the NOAA-9 AVHRR spectral channels 1 (0.568 - 0.698 μm) and 2 (0.704 - 0.990 μm) are not narrow bands and the radiative transfer code assumes monochromaticity, they were subdivided into segments. Channel 1 was divided into three bands centered at 0.595, 0.635, and 0.680 μm, whereas channel 2 was divided into four bands centered at 0.760, 0.840, 0.900, and 0.960 μm. Table 2.1 lists optical depth results for these wavelengths, as well as for the central wavelengths of the AVHRR bands as calculated by the moments method (Palmer and Tomasko, 1980).

Table 2.1 Optical depth results derived from atmospheric measurements at Edwards Air Force Base. Barometric pressure was measured at 963.03 mb on October 14 and 943.08 mb on May 5, and was assumed to be 943.08 on May 4.

Wavelength (micrometers)	Optical Depth			
	Total	Aerosol	Rayleigh	Ozone
October 14				
0.5950	0.1292	0.0299	0.0662	0.0330
0.6350	0.0995	0.0272	0.0508	0.0214
0.6800	0.0732	0.0247	0.0385	0.0100
0.7600	0.0495	0.0210	0.0246	0.0039
0.8400	0.0362	0.0182	0.0164	0.0015
0.9000	0.0289	0.0165	0.0124	0.0000
0.9600	0.0246	0.0150	0.0096	0.0000
0.6329	0.1011	0.0274	0.0505	0.0222
0.8471	0.0352	0.0180	0.0159	0.0014
May 4				
0.5950	0.1796	0.0740	0.0649	0.0407
0.6350	0.1468	0.0706	0.0498	0.0264
0.6800	0.1172	0.0672	0.0377	0.0123
0.7600	0.0909	0.0620	0.0241	0.0048
0.8400	0.0757	0.0577	0.0161	0.0019
0.9000	0.0670	0.0549	0.0122	0.0000
0.9600	0.0618	0.0524	0.0094	0.0000
0.6329	0.1486	0.0708	0.0505	0.0273
0.8471	0.0746	0.0573	0.0155	0.0017
May 5				
0.5950	0.2425	0.1401	0.0649	0.0375
0.6350	0.2096	0.1355	0.0498	0.0243
0.6800	0.1799	0.1309	0.0377	0.0113
0.7600	0.1521	0.1236	0.0241	0.0045
0.8400	0.1353	0.1175	0.0161	0.0018
0.9000	0.1256	0.1134	0.0122	0.0000
0.9600	0.1191	0.1097	0.0094	0.0000
0.6329	0.2114	0.1357	0.0505	0.0252
0.8471	0.1340	0.1170	0.0155	0.0016

3. Surface Reflectance Determination

(i) Pixel Area Measurements

Reflectance factor measurements were made on the dry lakebed at EAFB on October 14, 1986, May 5, 1987, and May 6, 1987. On October 14 and May 5, data were collected over a target area related to AVIRIS overflights. The target consisted of 64 20-meter pixels configured in a 16 by 4 pixel rectangle. The long side of the rectangle was oriented 10 degrees west of north. Ground spectral data were collected using two radiometers: a Barnes MMR (8 bands) and an Exotech (4 bands), both collecting data in spectral bands similar to the Landsat TM bandpasses. The instruments were suspended about 2 meters above ground by attachment to a backpack frame. The operators walked along a transect intersecting pixel centers and collected 8 samples per pixel with each instrument. These 8 readings were then averaged and a single reflectance factor determined for each pixel. The MMR was carried along the primarily north-south transects and the Exotech along the primarily east-west transects.

On May 6, data were collected in a similar manner over a target area related to a Landsat TM overpass. The TM target consisted of 64 30-meter pixels configured in a 16 by 4 pixel rectangle and oriented 9 degrees east of north. Twelve readings were collected along a transect through each pixel. The MMR was carried along the primarily east-west transect and the Exotech along the primarily north-south transect.

Weather on all three days was clear and the sun was never hidden by clouds throughout the measurement period. October 14 was an extremely clear day with a visibility calculated to be at least 300 km. There were no clouds on that day and on May 5, but a small growth of cumulus clouds was observed low on the horizon on May 6. There was also a significant amount of haze on the last day due to a nearby fire and smog.

Reflectance factors for all three dates were computed using the same barium sulfate panel (panel #11). For each instrument on each date, an average reflectance factor was computed for the entire 64-pixel site. The values from the MMR were used in this particular study because

they include more extensive wavelength coverage (Table 3.1). On all three days, the ground measurements were completed in less than one hour during the morning.

Table 3.1 Pixel area measurements of surface reflectance factor at Edwards Air Force Base. The reflectance factors are averages of the MMR data acquired over a 64 pixel site.

	October 14, 1986	May 5, 1987	May 6, 1987
Average solar zenith angle	44.5°	30.0°	30.0°
MMR band 1 (0.48223 μm)	0.2550	0.2566	0.2503
MMR band 2 (0.56137 μm)	0.3425	0.3361	0.3346
MMR band 3 (0.66021 μm)	0.4095	0.3969	0.4002
MMR band 4 (0.82138 μm)	0.4446	0.4272	0.4306
MMR band 5 (1.25405 μm)	0.4675	0.4450	0.4415
MMR band 6 (1.68790 μm)	0.4938	0.4673	0.4605
MMR band 7 (2.21736 μm)	0.4351	0.4090	0.3983

(ii) Bidirectional Reflectance Measurements

At a representative spot on the dry lakebed at EAFB, bidirectional reflectance measurements were made on May 5, 1987, May 6, 1987, and September 14, 1987. No effort was made to use exactly the same spot on all three dates, but the same general location was used each time. A special apparatus was used to measure surface reflectance factors at a number of view angles in a plane perpendicular to the SPOT satellite orbital path. More specifically, the set-up consisted of an arm to hold an Exotech radiometer at a distance of about 2.5 meters above the surface when in the vertical configuration. The arm could be tilted to provide view angles every 5 degrees from -45 to +45 degrees with respect to zenith. The apparatus was designed to measure the radiation from the same spot on the surface (± 2 cm) at all view angles. Each measurement sequence started at -45 degrees, proceeded to +45 degrees in 5 degree increments, and returned beginning with +45

back to -45 degrees. The two measurements for each angle were averaged, as were the times of the two measurements, to minimize variations due to changing solar zenith angle. Data collected with this instrument will hereafter be referred to as "BRF" data.

Several BRF data sets were obtained at various times on each of the three dates. Nadir reflectance factors from these measurement sets are listed in Table 3.2.

(iii) Surface Reflectance Estimates

Atmospheric radiative transfer computations require a surface reflectance value as one of the inputs at any given wavelength. The surface reflectance value should be appropriate for the solar zenith angle and the nadir view angle pertaining to the satellite sensor overpass of interest. Sun and view angle geometries for the NOAA-9 AVHRR overpasses of EAFB are given in Table 3.3. Because the reflectance data were acquired in TM bands, surface reflectance estimates were obtained in those bands first and later changed to values relevant to the first two AVHRR channels.

The pixel area measurements of surface reflectance at EAFB were made with nadir geometry and in the morning in support of different sensor overpasses, whereas the NOAA-9 AVHRR overpasses took place in the afternoon with the test site at off-nadir view angles. Therefore, the BRF data were used to adjust the pixel area reflectance values accordingly. An additional assumption is that the pixel area data are representative of an entire AVHRR picture element, which encompasses over one square kilometer (Table 3.3).

There are three steps involved in using the BRF data to obtain the proper surface reflectances (a detailed description may be found in Appendix A). First the nadir reflectance factors obtained during the bidirectional measurements (Table 3.2) are interpolated for the solar zenith angle at the time of NOAA-9 AVHRR overpasses. Secondly, an adjustment is made for the slight difference in surface reflectance between the pixel area site and the BRF site nearby. Finally, a view angle correction is made using BRF data for the appropriate solar zenith angle and nadir view angle, with a solar azimuth as close to the sensor view azimuth as possible. Tabulations of these adjustment steps are given in Table 3.4 for the first four TM bands.

Table 3.2 Nadir reflectance factors obtained during bidirectional reflectance measurements with an Exotech radiometer at Edwards Air Force Base.

Universal Time	Solar zenith (degrees)	Solar azimuth (degrees)	TM Band 1	TM Band 2	TM Band 3	TM Band 4
May 5, 1987						
15:21:15	61.9	89.2				
16:13:04	51.3	97.1	0.2443	0.3278	0.3903	0.4252
16:59:09	42.0	105.4	0.2491	0.3339	0.3976	0.4334
18:55:53	22.0	144.7				
22:16:02	27.1	232.1	0.2619	0.3471	0.4136	0.4494
23:22:00	39.0	251.5	0.2567	0.3398	0.4058	0.4401
May 6, 1987						
15:05:41	64.9	86.8	0.2428	0.3234	0.3849	0.4191
15:46:31	56.6	92.6	0.2451	0.3270	0.3901	0.4246
16:54:57	42.7	104.2	0.2492	0.3332	0.3963	0.4319
20:09:53	20.3	152.7	0.2693	0.3556	0.4235	0.4588
20:45:07	18.4	177.8	0.2702	0.3563	0.4244	0.4598
20:59:27	18.6	188.6	0.2698	0.3564	0.4246	0.4605
			HRV Band 1	HRV Band 2	HRV Band 3	
September 14, 1987						
15:53:09	62.5	106.3	0.2860	0.3690	0.4129	
16:02:38	60.6	108.0	0.2863	0.3701	0.4152	
16:39:49	53.5	115.2	0.2922	0.3794	0.4240	
17:15:32	47.2	123.3	0.2936	0.3815	0.4278	
17:35:50	43.8	128.6	0.2933	0.3811	0.4282	
18:00:01	40.1	135.8	0.2957	0.3843	0.4324	
18:22:20	37.2	143.3	0.2977	0.3871	0.4355	
18:38:49	35.3	149.5	0.2977	0.3868	0.4356	
18:51:44	34.1	154.8	0.2983	0.3891	0.4365	
19:14:08	32.5	164.6	0.2993	0.3952	0.4381	
19:40:45	31.6	177.0	0.3014	0.3938	0.4423	

Table 3.3 Sun and view angle geometries for the NOAA-9 AVHRR overpasses of EAFB. The nadir view angles are relative to vertical at ground level and view azimuth angles are in the satellite direction from the ground location (34° 57′ N, 117° 51′W).

Date	Overpass Time (U.T.)	Solar Zenith (Degrees)	Solar Azimuth (Degrees)	Solar Distance (A.U.)	Off-Nadir View (Degrees)	View Azimuth (Degrees)	Approximate Pixel Dimensions (km)
1986.10.14	21:46:55	53.0	221.6	0.9972	44.5	259	2.2 x 1.6
1987.05.04	22:29:54	40.7	252.8	1.0087	15.3	79	1.3 x 1.2
1987.05.05	22:19:03	38.5	250.8	1.0087	31.3	79	1.6 x 1.3

(iv) Change to AVHRR Channels

Since NOAA-9 AVHRR spectral channels 1 (570-700 nanometers) and 2 (714-983 nanometers) are not narrow bands and the Herman radiative transfer code assumes monochromaticity, they were subdivided into smaller segments. Channel 1 was divided into three bands centered at 595, 635, and 680 nm, whereas channel 2 was split into four bands centered at 760, 840, 900, and 960 nm. In order to run the Herman code at these seven wavelengths, the TM reflectance values obtained in the previous section were interpolated accordingly. However, because BRF data were only available in the first four TM bands, the surface reflectance factors computed in the previous section were limited to those bands and do not encompass the AVHRR channel segments at 900 and 960 nm. Therefore, estimates for MMR band 5 were also obtained (Appendix A), based on the relationship between MMR bands 5 and 4 as measured for the pixel area. It was then possible to interpolate at all seven AVHRR segment wavelengths, as well as at the central wavelengths of the two AVHRR channels (Table 3.5).

Table 3.4 Surface reflectance estimation for the EAFB pixel area site at the NOAA-9 AVHRR overpass. Solar zenith angle = θ_s; off-nadir view angle = θ_v (negative if satellite is viewing from East of the site). Details are discussed in Appendix A.

	TM Band 1	TM Band 2	TM Band 3	TM Band 4
October 14, 1986				
Nadir BRF (May 6) for θ_s = 53.0°	0.2462	0.3286	0.3917	0.4265
Site adjustment	1.0270	1.0304	1.0351	1.0313
	0.2528	0.3386	0.4055	0.4399
View adjustment (May 5 BRF)	1.3400	1.2900	1.2800	1.2310
for θ_v = +44.5°	0.3388	0.4368	0.5190	0.5415
May 4, 1987				
Nadir BRF (May 5 and 6) for θ_s = 40.7°	0.2506	0.3351	0.3989	0.4345
Site adjustment	0.9748	0.9715	0.9695	0.9600
	0.2443	0.3255	0.3867	0.4171
View adjustment (May 5 BRF)	0.9860	0.9820	0.9970	0.9800
for θ_v = -15.3°	0.2409	0.3197	0.3778	0.4088
May 5, 1987				
Nadir BRF (May 5) for θ_s = 38.5°	0.2521	0.3370	0.4014	0.4372
Site adjustment	0.9892	0.9756	0.9669	0.9572
	0.2494	0.3288	0.9881	0.4185
View adjustment (May 5 BRF)	1.0000	0.9860	0.9770	0.9760
for θ_v = -31.3°	0.2494	0.3242	0.3792	0.4084

Table 3.5 Surface reflectance factors in the seven AVHRR channel segments based on wavelength interpolations of the adjusted TM band values (also listed).

Center Wavelength (Micrometers)	October 14, 1986	May 4, 1987	May 5, 1987
0.48223 (TM Band 1)	0.3388	0.2409	0.2494
0.56137 (TM Band 2)	0.4369	0.3197	0.3242
0.66021 (TM Band 3)	0.5198	0.3778	0.3791
0.82138 (TM Band 4)	0.5415	0.4088	0.4084
1.25405 (MMR Band 5)	0.5694	0.4259	0.4255
0.595 (AVHRR Channel 1, Segment 1)	0.4648	0.3395	0.3429
0.635 (AHVRR Channel 1, Segment 2)	0.4981	0.3630	0.3651
0.680 (AHVRR Channel 1, Segment 3)	0.5218	0.3816	0.3827
0.760 (AHVRR Channel 2, Segment 1)	0.5329	0.3910	0.3973
0.840 (AHVRR Channel 2, Segment 2)	0.5427	0.4096	0.4091
0.900 (AHVRR Channel 2, Segment 3)	0.5466	0.4119	0.4115
0.960 (AHVRR Channel 2, Segment 4)	0.5504	0.4143	0.4139
0.63288 (AVHRR Channel 1)	0.4963	0.3617	0.3639
0.84709 (AVHRR Channel 2)	0.5431	0.4098	0.4094

4. Radiative Transfer Computations

Atmospheric parameters (Section 2) and ground reflectances (Section 3) for the seven wavelengths were input to the Herman radiative transfer code (Herman and Browning, 1975). Output from the code includes radiance at the entrance aperture of the AVHRR sensor, normalized for unity exo-atmospheric solar irradiance. For use in the code, the atmosphere is divided into a sufficient number of plane-parallel layers such that changes within each layer are due only to single-scattering processes. The Gauss-Seidel iterative technique is used to solve the equation of radiative transfer. Upon convergence, all multiple scattering effects have been taken into account. Values of 5.02, 0.02, and 0.04 μm were used for the maximum and minimum radii and incremental step size, respectively, for the aerosols. A vertical aerosol distribution as measured by Elterman (1966) was assumed and the aerosols were given a refractive index of 1.54-0.01i. Other important inputs to the Herman code include the Rayleigh, aerosol, and ozone optical depth values, as well as the Junge parameter.

The spectral radiance is ultimately calculated as the product of the exo-atmospheric irradiance and the normalized radiance determined from the Herman code, divided by the square of the solar distance in astronomical units. The exo-atmospheric solar irradiance data are those recommended by Frohlich and published by Iqbal (1983). They represent a carefully edited combination of results published by Neckel and Labs, Thekaekara, Arvesen, and others. The values were adjusted to yield an integrated value of 1367 Wm^{-2}, the solar constant as proposed by the World Radiation Center.

In order to combine the code spectral radiance results for the narrower bands, weighting coefficients were determined from the areas under selected intervals of the relative spectral response profiles, $R(\lambda)$, for each AVHRR band. For example, the weighting coefficient for 595 nm is given by

$$\frac{\int_{530}^{610} R(\lambda)d\lambda}{\int_{530}^{800} R(\lambda)d\lambda} .$$

The code spectral radiance in each AVHRR band is then the weighted sum of code spectral radiances for the narrower bands. For comparison, the code spectral radiance was also determined from Herman code computations at the central wavelengths of AVHRR channels 1 and 2.

A final adjustment is applied to the code spectral radiances to correct for gaseous absorption. The Herman code takes into account ozone optical depth but does not consider H_2O, CO_2, and O_2 transmittance. In AVHRR band 2 especially, there is significant absorption around 0.94 μm due to water vapor and around 0.76 μm due to oxygen. Thus the "5-S" atmospheric program of Tanré et al. (1985) is run to obtain the total gaseous transmittance due to the four gases (H_2O, O_3, CO_2, O_2). The final radiance values predicted at the AVHRR sensor are the product of total gas transmittance except ozone and the code spectral radiance.

5. Image Data Manipulation

Bright and dark features were identified in SPOT HRV and AVIRIS imagery (Vane, 1987), acquired at other times for the EAFB area, that were also distinguishable in the AVHRR scenes. The features used for this purpose were not likely to have changed places in time and were sufficiently numerous to minimize the effect of systematic geometric distortions. The location of the ground measurement site on the dry lakebed could then be estimated visually in the AVHRR imagery using relative distances and triangulation. Digital image analysis facilities were used for this purpose. The corresponding digital counts were then interpolated from the image values in channels 1 and 2 (Figure 5.1). The results are given in Table 5.1 and are denoted as "best estimate".

The surface at Rogers Lake is quite flat for many kilometers in all directions but its reflectance characteristics are reasonably uniform only in a limited area, roughly 1 3/4 kilometers in the predominantly East-West direction and roughly double that distance in the predominantly North-South direction. Thus, although that part of the dry lakebed provides a large uniform target for high-resolution sensors, it can accommodate the area of only one AVHRR pixel (the approximate pixel dimensions on the various dates are listed in Table 3.3). Because this site is not easy to pinpoint in the AVHRR imagery, digital counts were also obtained for locations plus or minus half a pixel away in the direction of the strongest radiance gradient (Table 5.1).

Figure 5.1 Digital counts (10-bit scale) of NOAA-9 AVHRR channels 1 and 2 at Edwards Air Force Base for three dates. In each case, the dot indicates the estimated location of the ground measurement site. Since the off-nadir view angle differed from date to date, the digital counts correspond to different pixel sizes on different dates (Table 2.3).

	AVHRR Channel 1					AVHRR Channel 2				
	126	147	176	184	169	143	160	184	191	180
	147	196	203	192	181	159	203	208	196	189
October 14, 1986	173	221	202	188	189	184	227	207	191	197
	205	225	196	184	185	210	230	201	188	190
	211	221	195	181	184	216	226	200	186	188
	190	213	196	186	189	198	220	200	192	194
	188	224	233	224	225	202	235	242	232	232
	251	249	230	217	214	262	258	238	225	221
May 4, 1987	266	246	232	218	213	275	255	240	226	220
	268	247	231	220	224	277	256	239	227	230
	266	251	237	224	224	276	260	245	230	231
	257	247	232	222	224	266	255	240	229	230
	180	216	232	227		193	227	240	235	
	238	256	232	217		249	265	241	225	
May 5, 1987	268	253	230	216		277	263	238	222	
	278	252	230	223		286	261	238	229	
	271	255	236	226		280	263	243	232	

Table 5.1 Digital counts (10-bit scale) from the NOAA-9 AVHRR imaging the dry lakebed at EAFB on three dates. The best estimate is the value corresponding to the area where ground reflectance measurements were made. Because this area is not easy to pin-point, digital counts were also obtained plus or minus half a pixel away in the direction of the strongest radiance gradient.

	AVHRR Channel 1	AVHRR Channel 2
Central wavelength (micrometers)	0.63288	0.84709
October 14, 1986 digital counts:		
Best estimate	199.00	204.00
Half-pixel shifts in "East-West" direction	192.50 211.00	196.75 216.25
May 4, 1987 digital counts:		
Best estimate	231.50	239.50
Half-pixel shifts in "East-West" direction	225.25 239.00	233.00 247.50
May 5, 1987 digital counts:		
Best estimate	241.25	250.00
Half-pixel shifts in "East-West" direction	230.00 252.50	238.00 262.00

6. Calibration of AVHRR Channels 1 and 2

A prelaunch calibration of the reflective channels of the NOAA-9 AVHRR was obtained from Smith (1987) (Table 6.0). It can be represented by

$$L_1 = 0.05246\ D_1 - 2.0465$$

and

$$L_2 = 0.03363\ D_2 - 1.3440,$$

where radiance L is in units of $mWcm^{-2}sr^{-1}\mu m^{-1}$, D represents digital counts, and the subscripts 1 and 2 identify AVHRR channels 1 and 2, respectively. Both relations are highly linear, with r^2 values of 0.999999.

In-orbit calibration results from the present methodology are given in Tables 6.1 - 6.3 for October 14, 1986, Table 6.4 - 6.6 for May 4, 1987, and Tables 6.7 - 6.9 for May 5, 1987. The first of three tables for each date concerns results for channel 1 based on three narrower bands, the second table concerns channel 2 based on four narrower bands, and the third table presents results for channels 1 and 2 without subdivision. Calibration coefficients are presented in terms of counts per unit radiance and three values are given in each case, corresponding to the best estimate and results for locations plus or minus half a pixel to either side in the scan direction (as discussed in Section 5). Note that in these tables, radiance values are given in $Wm^{-2}sr^{-1}\mu m^{-1}$.

It is evident from the Tables 6.1-6.9 that the results based on narrower bands differ somewhat from those for the corresponding channels without subdivision. A study to assess the validity of band subdivision for the purposes of running monochromatic radiative transfer codes is currently in progress. Preliminary results indicate that it is better to use the Palmer central wavelength rather than subdividing AVHRR channels into a few segments. Thus, for the purposes of discussion, the results based on single wavelength calculations only will be considered.

The calibration results can also be expressed in terms of gain. Based on space views taken by the sensor, the number of digital counts corresponding to zero radiance has remained fairly constant with time for the AVHRR sensors (Frouin and Gautier, 1987; Markham, 1988). For the NOAA-9 AVHRR, prelaunch digital count values are 39 and 40 for channels 1 and 2, respectively

(Table 6.0). Thus, a gain coefficient is obtained by dividing predicted radiance by the corresponding digital image count from which the dark count has been subtracted; i.e., gain = predicted radiance/(digital image count - dark image count).

Absolute calibration gain coefficients for the reflective channels of the NOAA-9 AVHRR are listed in Table 6.10 and portrayed as a function of time in Figures 6.1 and 6.2. Results (slightly revised) from a Method 1 analysis on August 28, 1985 at White Sands (Slater et al., 1987b) are also included. Clearly, the sensor's responsivity has degraded significantly with time, with the greater change occurring in channel 2. That the gain coefficients in October 1986 should be somewhat higher than in May 1987 is largely due to the difficulty in making a precise BRF correction for the earlier date when the nadir view angle was nearly 45 degrees, but also partly due to the problem of having a 2.2 kilometer pixel dimension in the scan line direction, which exceeds the size of the uniform reflectance patch at EAFB. The results for May 4 and May 5, 1987, are reasonably consistent. Although the same surface reflectance measurements were used for both days since no reflectance measurements were made on May 4th, different atmospheric parameters were used and the off-nadir view angles differed considerably.

Table 6.0. Prelaunch calibration for the NOAA-9 AVHRR sensor (Smith, 1987). Radiance values are in units of $mWcm^{-2}sr^{-1}\mu m^{-1}$. Digital counts are on a 10-bit scale.

Channel 1		Channel 2	
Counts	Radiance	Counts	Radiance
812	40.55	940	30.27
745	37.04	789	25.19
683	33.78	640	20.18
618	30.37	484	14.93
551	26.86	332	9.82
485	23.40	179	4.68
421	20.04	40	0.00
357	16.68		
294	13.38		
227	9.86		
161	6.40		
97	3.04		
39	0.00		

Table 6.1 Calibration of NOAA-9 AVHRR Channel 1 at EAFB on October 14, 1986.

Solar Zenith Angle: 53.00	Time of Overpass: 21:46:55 (UT)
Solar Azimuth Angle: 221.60	Location: EAFB Mojave, CA.
Solar Distance (AU): 0.9972	Latitude: 34 deg. 58 min.
Junge Size Distribution: 4.040	Longitude: 117 deg. 51 min.
Aerosol Size Range: 0.02 to 5.02 μm	NOAA Zenith Angle: 44.50
Refractive Index: 1.54 - 0.01 i	NOAA Azimuth Angle: 255.00
Calculated Visibility: 300 km	Relative Azimuth Angle: 33.40

Wavelength in nm	595	635	680
Bandwidth	530-610	610-660	660-800
Mie Optical Depth	0.0299	0.0272	0.0247
Rayleigh Optical Depth	0.0662	0.0508	0.0385
Ozone Optical Depth	0.0330	0.0214	0.0100
Spectral Reflectance	0.3932	0.4195	0.4388
Exoatmospheric E0 (W/m2.μm)	1785	1630	1473
Normalized Code Radiance	0.0744	0.0790	0.0824
Spectral Radiance	133.60	129.43	122.00
Weighting Coefficients	0.2912	0.3677	0.3411
Weighted Spectral Radiance	38.90	47.59	41.61

Central Wavelength (μm):		0.63288	
Code Spectral Radiance (W/m2.μm.sr):		128.11	
Total Gaseous Transmittance:		0.9200	
Radiance Predicted at the Sensor (Pcode):		117.86	
Image Digital Counts (10-bit scale):		199.00	192.50 211.00
Spectral Radiance from Preflight Calibration:		83.93	80.52 90.23
Pcode Counts Per Unit Radiance:		1.69	1.63 1.79
Preflight Counts Per Unit Radiance:		2.37	2.39 2.34
(Pcode-Pre)/Pre (%)(radiance):		40.43	46.37 30.63

Table 6.2 Calibration of NOAA-9 AVHRR Channel 2 at EAFB on October 14, 1986.

Solar Zenith Angle: 53.00	Time of Overpass: 21:46:55 (UT)
Solar Azimuth Angle: 221.60	Location: EAFB Mojave, CA.
Solar Distance (AU): 0.9972	Latitude: 34 deg. 58 min.
Junge Size Distribution: 4.040	Longitude: 117 deg. 51 min.
Aerosol Size Range: 0.02 to 5.02 μm	NOAA Zenith Angle: 44.50
Refractive Index: 1.54 - 0.01 i	NOAA Azimuth Angle: 255.00
Calculated Visibility: 300 km	Relative Azimuth Angle: 33.40

Wavelength in nm	760	840	900	960
Bandwidth	680-800	800-870	870-950	950-1160
Mie Optical Depth	0.0210	0.0182	0.0165	0.0150
Rayleigh Optical Depth	0.0246	0.0164	0.0124	0.0096
Ozone Optical Depth	0.0039	0.0015	0.0000	0.0000
Spectral Reflectance	0.4496	0.4627	0.4782	0.4936
Exoatmospheric E0 (W/m2.μm)	1222.5	1020.0	913.0	771.0
Normalized Code Radiance	0.0844	0.0869	0.0899	0.0929
Spectral Radiance	103.79	89.17	82.53	72.00
Weighting Coefficients	0.3403	0.2601	0.2728	0.1268
Weighted Spectral Radiance	35.32	23.19	22.51	9.13

Central Wavelength (μm):	0.84709		
Code Spectral Radiance (W/m2.μm.sr):	90.16		
Total Gaseous Transmittance:	0.8880		
Radiance Predicted at the Sensor (Pcode):	80.06		
Image Digital Counts (10-bit scale):	204.00	196.75	216.25
Spectral Radiance from Preflight Calibration:	55.17	52.73	59.28
Pcode Counts Per Unit Radiance:	2.55	2.46	2.70
Preflight Counts Per Unit Radiance:	3.70	3.73	3.65
(Pcode-Pre)/Pre (%)(radiance):	45.13	51.84	35.04

Table 6.3 Calibration of NOAA-9 AVHRR Channels 1 and 2 (without subdivision) at EAFB on October 14, 1986.

Solar Zenith Angle: 53.00	Time of Overpass: 21:46:55 (UT)					
Solar Azimuth Angle: 221.60	Location: EAFB Mojave, CA.					
Solar Distance (AU): 0.9972	Latitude: 34 deg. 58 min.					
Junge Size Distribution: 4.040	Longitude: 117 deg. 51 min.					
Aerosol Size Range: 0.02 to 5.02 μm	NOAA Zenith Angle: 44.50					
Refractive Index: 1.54 - 0.01 i	NOAA Azimuth Angle: 255.00					
Calculated Visibility: 300 km	Relative Azimuth Angle: 33.40					
Wavelength in nm	632.88			847.09		
Bandwidth	568-698			704-990		
Mie Optical Depth	0.0274			0.0180		
Rayleigh Optical Depth	0.0515			0.0159		
Ozone Optical Depth	0.0222			0.0014		
Spectral Reflectance	0.4182			0.4645		
Exoatmospheric E0 (W/m2.μm)	1544			999.2		
Normalized Code Radiance	0.0787			0.0863		
Spectral Radiance	122.19			86.73		
Weighting Coefficients	1.0000			1.0000		
Weighted Spectral Radiance	122.19			86.73		
Central Wavelength (μm):	0.63288			0.84709		
Code Spectral Radiance (W/m2.μm.sr):	122.19			86.73		
Total Gaseous Transmittance:	0.9200			0.8880		
Predicted Sensor Radiance (Pcode):	112.41			77.02		
Image Digital Counts (10-bit scale):	199.00	192.50	211.00	204.00	196.75	216.25
Spectral Radiance from Preflight Cal:	83.93	80.52	90.23	55.17	52.73	59.28
Pcode Counts Per Unit Radiance:	1.77	1.71	1.88	2.65	2.55	2.81
Preflight Counts Per Unit Radiance:	2.37	2.39	2.34	3.70	3.73	3.65
(Pcode-Pre)/Pre (%)(radiance):	33.94	39.61	24.59	39.61	46.07	29.91

Table 6.4 Calibration of NOAA-9 AVHRR channel 1 at EAFB on May 4, 1987.

Solar Zenith Angle: 40.70	Time of Overpass: 22:29:54 (UT)
Solar Azimuth Angle: 252.80	Location: EAFB Mojave, CA.
Solar Distance (AU): 1.0087	Latitude: 34 deg. 58 min.
Junge Size Distribution: 2.723	Longitude: 117 deg. 51 min.
Aerosol Size Range: 0.02 to 5.02 μm	NOAA Zenith Angle: 15.38
Refractive Index: 1.54 - 0.01 i	NOAA Azimuth Angle: 81.70
Calculated Visibility: 68 km	Relative Azimuth Angle: -171.10

Wavelength in nm	595	635	680
Bandwidth	530-610	610-660	660-800
Mie Optical Depth	0.0740	0.0706	0.0672
Rayleigh Optical Depth	0.0649	0.0498	0.0377
Ozone Optical Depth	0.0407	0.0264	0.0123
Spectral Reflectance	0.3395	0.3630	0.3816
Exoatmospheric E0 (W/m2.μm)	1785	1630	1473
Normalized Code Radiance	0.0832	0.0880	0.0919
Spectral Radiance	146.00	140.99	133.00
Weighting Coefficients	0.2912	0.3677	0.3411
Weighted Spectral Radiance	42.52	51.84	45.37

Central Wavelength (μm):	0.63288		
Code Spectral Radiance (W/m2.μm.sr):	139.73		
Total Gaseous Transmittance:	.9290		
Radiance Predicted at the Sensor (Pcode):	129.80		
Image Digital Counts (10-bit scale):	231.50	225.25	239.00
Spectral Radiance from Preflight Calibration:	100.98	97.70	104.91
Pcode Counts Per Unit Radiance:	1.78	1.74	1.84
Preflight Counts Per Unit Radiance:	2.29	2.31	2.28
(Pcode-Pre)/Pre (%)(radiance):	28.54	32.86	23.72

Table 6.5 Calibration of NOAA-9 AVHRR Channel 2 at EAFB on May 4, 1987.

Solar Zenith Angle: 40.70
Solar Azimuth Angle: 252.80
Solar Distance (AU): 1.0087
Junge Size Distribution: 2.723
Aerosol Size Range: 0.02 to 5.02 μm
Refractive Index: 1.54 - 0.01 i
Calculated Visibility: 68 km

Time of Overpass: 22:29:54 (UT)
Location: EAFB Mojave, CA.
Latitude: 34 deg. 58 min.
Longitude: 117 deg. 51 min.
NOAA Zenith Angle: 15.38
NOAA Azimuth Angle: 81.70
Relative Azimuth Angle: -171.10

Wavelength in nm Bandwidth	760 680-800	840 800-870	900 870-50	960 950-160
Mie Optical Depth	0.0620	0.0577	0.0549	0.0524
Rayleigh Optical Depth	0.0241	0.0161	0.0122	0.0094
Ozone Optical Depth	0.0048	0.0019	0.0000	0.0000
Spectral Reflectance	0.3970	0.4096	0.4119	0.4143
Exoatmospheric E0 (W/m2.μm)	1222.5	1020.0	913.0	771.0
Normalized Code Radiance	0.0951	0.0978	0.0983	0.0988
Spectral Radiance	114.29	98.08	88.21	74.90
Weighting Coefficients	0.3403	0.2601	0.2728	0.1268
Weighted Spectral Radiance	38.89	25.51	24.06	9.50

Central Wavelength (μm):	0.84709		
Code Spectral Radiance (W/m2.μm.sr):	97.96		
Total Gaseous Transmittance:	0.9110		
Radiance Predicted at the Sensor (Pcode):	89.25		
Image Digital Counts (10-bit scale):	239.50	233.00	247.50
Spectral Radiance from Preflight Calibration:	67.10	64.92	69.79
Pcode Counts Per Unit Radiance:	2.68	2.61	2.77
Preflight Counts Per Unit Radiance:	3.57	3.59	3.55
(Pcode-Pre)/Pre (%)(radiance):	33.00	37.47	27.87

Table 6.6 Calibration of NOAA-9 AVHRR Channesl 1 and 2 (without subdivision) at EAFB on May 4, 1987.

Solar Zenith Angle: 40.70
Solar Azimuth Angle: 252.80
Solar Distance (AU): 1.0087
Junge Size Distribution: 2.723
Aerosol Size Range: 0.02 to 5.02 μm
Refractive Index: 1.54 - 0.01 i
Calculated Visibility: 300 km

Time of Overpass: 22:29:54 (UT)
Location: EAFB Mojave, CA.
Latitude: 34 deg. 58 min.
Longitude: 117 deg. 51 min.
NOAA Zenith Angle: 15.30
NOAA Azimuth Angle: 81.70
Relative Azimuth Angle: -171.10

Wavelength in nm	632.88			847.09		
Bandwidth	568-698			704-990		
Mie Optical Depth	0.0708			0.0573		
Rayleigh Optical Depth	0.0505			0.0155		
Ozone Optical Depth	0.273			0.0017		
Spectral Reflectance	0.3617			0.4098		
Exoatmospheric E0 (W/m2.μm)	1544			999.2		
Normalized Code Radiance	0.0877			0.0975		
Spectral Radiance	133.14			95.76		
Weighting Coefficients	1.0000			1.0000		
Weighted Spectral Radiance	133.14			95.76		
Central Wavelength (μm):	0.63288			0.84709		
Code Spectral Radiance (W/m2.μm.sr):	133.14			95.76		
Total Gaseous Transmittance:	0.9290			0.9110		
Predicted Sensor Radiance (Pcode):	123.69			87.24		
Image Digital Counts (10-bit scale):	231.50	225.25	239.00	239.50	233.00	247.50
Spectral Radiance from Preflight Cal:	100.98	97.70	107.91	67.10	64.92	69.79
Pcode Counts Per Unit Radiance:	1.87	1.82	1.93	2.75	2.67	2.84
Preflight Counts Per Unit Radiance:	2.29	2.31	2.28	3.57	3.59	3.55
(Pcode-Pre)/Pre (%)(radiance):	22.48	26.60	17.89	30.01	34.39	25.00

Table 6.7 Calibration of NOAA-9 AVHRR Channel 1 at EAFB on May 5, 1987.

Solar Zenith Angle: 38.50	Time of Overpass: 22:19:03 (UT)
Solar Azimuth Angle: 250.80	Location: EAFB Mojave, CA.
Solar Distance (AU): 1.0087	Latitude: 34 deg. 58 min.
Junge Size Distribution: 2.511	Longitude: 117 deg. 51 min.
Aerosol Size Range: 0.02 to 5.02 μm	NOAA Zenith Angle: 31.30
Refractive Index: 1.54 - 0.01 i	NOAA Azimuth Angle: 81.70
Calculated Visibility: 68 km	Relative Azimuth Angle: -169.10

Wavelength in nm	595	635	680
Bandwidth	530-610	610-660	660-800
Mie Optical Depth	0.1401	0.1355	0.1309
Rayleigh Optical Depth	0.0649	0.0498	0.0377
Ozone Optical Depth	0.0375	0.0243	0.0113
Spectral Reflectance	0.3429	0.3651	0.3827
Exoatmospheric E0 (W/m2.μm)	1785	1630	1473
Normalized Code Radiance	0.0873	0.0915	0.0950
Spectral Radiance	153.15	146.64	137.54
Weighting Coefficients	0.2912	0.3677	0.3411
Weighted Spectral Radiance	44.60	53.92	46.91

Central Wavelength (μm):	0.63288		
Code Spectral Radiance (W/m2.μm.sr):	145.43		
Total Gaseous Transmittance:	0.9260		
Radiance Predicted at the Sensor (Pcode):	134.67		
Image Digital Counts (10-bit scale):	241.25	230.00	252.50
Spectral Radiance from Preflight Calibration:	106.09	100.19	112.00
Pcode Counts Per Unit Radiance:	1.79	1.71	1.87
Preflight Counts Per Unit Radiance:	2.27	2.30	2.25
(Pcode-Pre)/Pre (%)(radiance):	26.93	34.41	20.24

Table 6.8 Calibration of NOAA-9 AVHRR Channel 2 at EAFB on May 5, 1987.

Solar Zenith Angle: 38.50	Time of Overpass: 22:19:03 (UT)
Solar Azimuth Angle: 250.80	Location: EAFB Mojave, CA.
Solar Distance (AU): 1.0087	Latitude: 34 deg. 58 min.
Junge Size Distribution: 2.511	Longitude: 117 deg. 51 min.
Aerosol Size Range: 0.02 to 5.02 μm	NOAA Zenith Angle: 31.38
Refractive Index: 1.54 - 0.01 i	NOAA Azimuth Angle: 81.70
Calculated Visibility: 68 km	Relative Azimuth Angle: -169.10

Wavelength in nm	760	840	900	960
Bandwidth	680–800	800–870	870–950	950–1160
Mie Optical Depth	0.1236	0.1175	0.1134	0.1097
Rayleigh Optical Depth	0.0241	0.0161	0.0122	0.0094
Ozone Optical Depth	0.0045	0.0018	0.0000	0.0000
Spectral Reflectance	0.3973	0.4091	0.4115	0.4139
Exoatmospheric E0 (W/m2.μm)	1222.5	1020.0	913.0	771.0
Normalized Code Radiance	0.0980	0.1005	0.1010	0.1016
Spectral Radiance	117.71	100.79	90.67	76.98
Weighting Coefficients	0.3403	0.2601	0.2728	0.1268
Weighted Spectral Radiance	40.06	26.21	24.73	9.76

Central Wavelength (μm):	0.84709		
Code Spectral Radiance (W/m2.μm.sr):	100.77		
Total Gaseous Transmittance:	0.9090		
Radiance Predicted at the Sensor (Pcode):	91.60		
Image Digital Counts (10-bit scale):	250.00	238.00	262.00
Spectral Radiance from Preflight Calibration:	70.64	66.60	74.67
Pcode Counts Per Unit Radiance:	2.73	2.60	2.86
Preflight Counts Per Unit Radiance:	3.54	3.57	3.51
(Pcode-Pre)/Pre (%)(radiance):	29.68	37.53	22.67

Table 6.9 Calibration of NOAA-9 AVHRR Channels 1 and 2 (without subdivision) at EAFB on May 5, 1987.

Solar Zenith Angle: 38.00	Time of Overpass: 22:19:03(UT)
Solar Azimuth Angle: 250.80	Location: EAFB Mojave, CA.
Solar Distance (AU): 2.511	Latitude: 34 deg. 58 min.
Junge Size Distribution: 2.511	Longitude: 117 deg. 51 min.
Aerosol Size Range: 0.02 to 5.02 μm	NOAA Zenith Angle: 31.30
Refractive Index: 1.54 - 0.01 i	NOAA Azimuth Angle: 81.70
Calculated Visibility: 68 km	Relative Azimuth Angle: -169.10

Wavelength in nm	632.88			847.09		
Bandwidth	568-698			704-990		
Mie Optical Depth	0.1357			0.1170		
Rayleigh Optical Depth	0.0505			0.0155		
Ozone Optical Depth	0.0252			0.0016		
Spectral Reflectance	0.3639			0.4094		
Exoatmospheric E0 (W/m2.μm)	1544			999.2		
Normalized Code Radiance	0.0913			0.1006		
Spectral Radiance	138.54			98.79		
Weighting Coefficients	1.0000			1.0000		
Weighted Spectral Radiance	138.54			98.79		
Central Wavelength (μm):	0.63288			0.84709		
Code Spectral Radiance (W/m2.μm.sr):	138.54			98.79		
Total Gaseous Transmittance:	0.9260			0.9090		
Predicted Sensor Radiance (Pcode):	128.29			89.80		
Image Digital Counts (10-bit scale):	241.25	230.00	252.50	250.00	238.00	262.00
Spectral Radiance from Preflight Cal:	106.09	100.19	112.00	70.64	66.60	74.67
Pcode Counts Per Unit Radiance:	1.88	1.79	1.97	2.78	2.65	2.92
Preflight Counts Per Unit Radiance:	2.27	2.30	2.25	3.54	3.57	3.51
(Pcode-Pre)/Pre (%)(radiance):	20.92	28.04	14.55	27.13	34.83	20.26

Table 6.10. NOAA-9 AVHRR radiometric calibration results. For Method 2 at EAFB, results are given in parentheses for locations plus or minus half a pixel away in the scan direction. Gain coefficients are in units of $Wm^{-2}sr^{-1}\mu m^{-1}count^{-1}$.

Date	Method	Channel 1 Gain	Difference from Prelaunch	Channel 2 Gain	Difference from Prelaunch
Prelaunch		0.5243		0.3286	
1985.08.28	1	0.552	5.2%	0.390	18.7%
1986.10.14	2	0.703 (0.654, 0.732)	34.1%	0.470 (0.437, 0.491)	43.0%
1987.05.04	2	0.674 (0.649, 0.697)	28.6%	0.447 (0.430, 0.462)	36.0%
1987.05.05	2	0.666 (0.631, 0.705)	27.0%	0.436 (0.413, 0.463)	32.7%

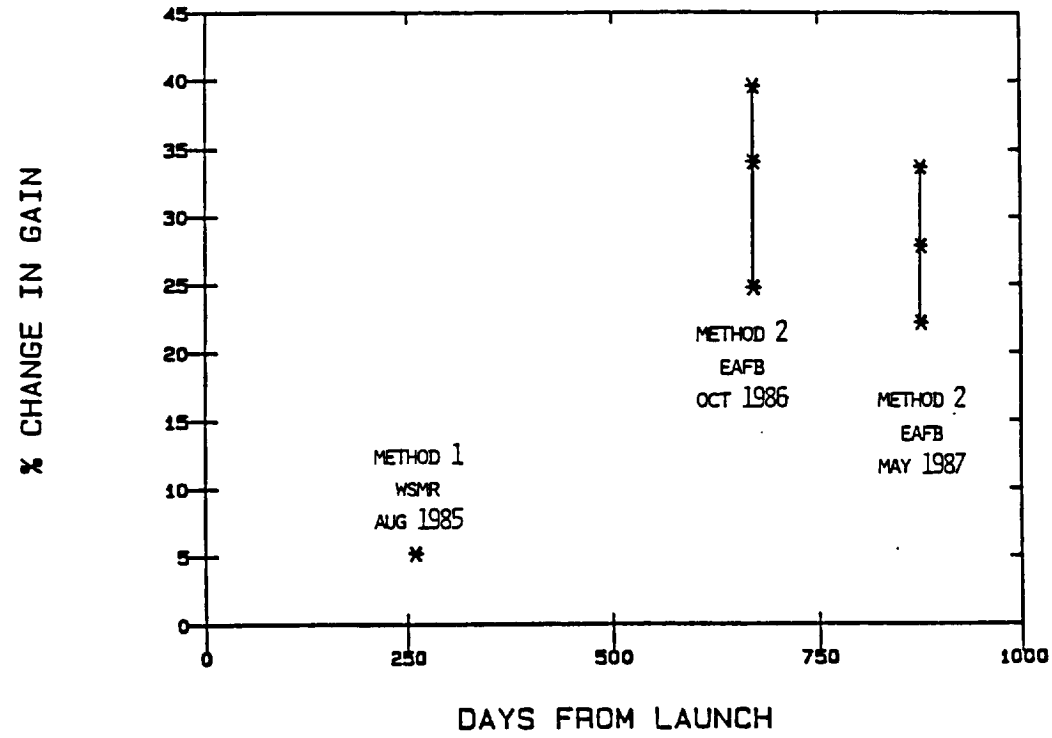

Figure 6.1. NOAA-9 AVHRR channel 1 calibration results expressed as percent change in gain as a function of time. In Method 2 cases at EAFB, results for locations plus or minus half a pixel away in the scan direction give rise to the error bars. The May 1987 results are averages from May 4 and May 5.

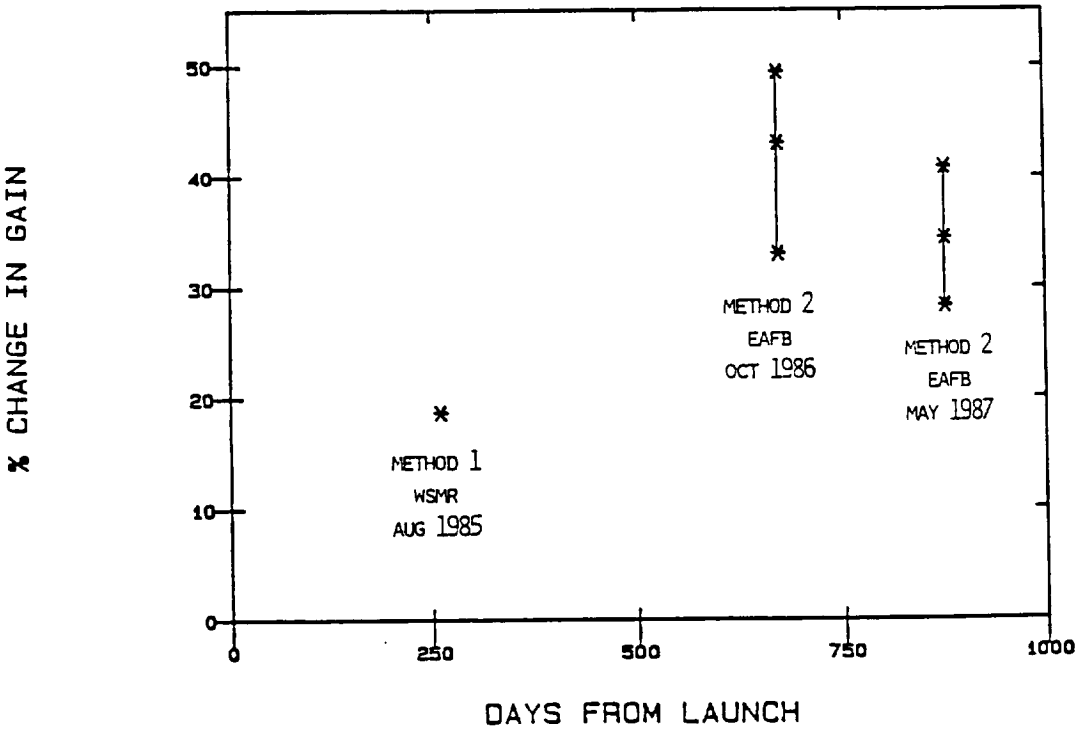

Figure 6.2. As for Figure 6.1, except for NOAA-9 AVHRR channel 2.

7. Concluding Remarks

A significant degradation in NOAA-9 AVHRR responsivity has occurred since the prelaunch calibration and with time since launch. As of May 1987, the change has been on the order of 25 to 30 percent in channel 1 and approximately 35 percent in channel 2. The analysis of more recent data sets is needed to update and further characterize the degradation. In this regard, a data set involving TM, HRV, and AVHRR imagery is currently being assembled after a successful field trip to White Sands on February 8-10, 1988.

There are some limitations to the use of Method 2 at the Rogers (dry) Lake site at Edwards Air Force Base. The uniform area is limited to one AVHRR pixel and is surrounded by terrain of much brighter and much darker reflectance on either side. In addition, unlike the gypsum at White Sands, the surface is not very lambertian so that BRF corrections are important. (It should also be noted that the radiative transfer codes assume lambertian reflectance.) Method 2 using the Rogers (dry) Lake site is not likely to be able to track gain changes less than about 10 percent.

8. References

Elterman. L. (1966), Aerosol measurements in the troposphere and stratosphere, Appl. Opt., 5:1769-1776.

Frouin, R., and Gautier, C. (1987), Calibration and NOAA-7 AVHRR, GOES-5, and GOES-6 VISSR/VAS solar channels, Remote Sens. Environ., 22:73-101.

Herman, B. M. and Browning, S. R. (1975) The effect of aerosols on the earth-atmosphere albedo, J. Atmos. Sci., 22:158-165.

Iqbal, M. (1983), An Introduction to Solar Radiation, Academic Press, New York.

Junge, C. E. (1963), Air Chemistry and Radioactivity, Academic Press, New York.

Markham, B. L. (1988), communication to the authors.

Palmer, J. M., and Tomasko, M. G. (1980), Broadband radiometry with spectrally selective detectors, Optics Letters, 5:208-210.

Slater, P. N., Biggar, S. F., Holm, R. G., Jackson, R. D., Mao, Y., Moran, M. S., Palmer, J. M. and Yuan, B. (1987a), Reflectance- and radiance-based methods for the in-flight absolute calibration of multispectral sensors, Remote Sens. Environ., 22:11-37.

Slater, P. N. Teillet, P. M., and Mao, Y. (1987b), The absolute radiometric calibration of the Advanced Very High Resolution Radiometer, Semi-Annual Status Report, NASA Grant NAG5-859, Optical Sciences Center, University of Arizona, Tucson, Arizona, 26 pages.

Smith, G. R. (1987), communication to the authors.

Tanré, D., Deroo, C., Duhaut, P., Herman, M., Morcrette, J. J., Perbos, J., and Deschamps, P. Y. (1985), Effets atmosphériques en télédétection--logiciel de simulation du signal satellitaire dans le spectre solaire, Proc. Third Int. Colloq. on Spectral Signatures of Objects in Remote Sensing, ESA SP-247, pp. 315-319.

9. Appendix

Surface Reflectance Estimations at EAFB

Recall that pixel area measurements were made on the mornings of October 14, 1986, May 4, 1987, and May 5, 1987, and that BRF data were acquired at several times on May 5, 1987, May 6, 1987, and September 14, 1987. The objective here is to estimate reflectance factors for the pixel area surface at the time of NOAA-9 AVHRR overpass in the afternoon.

(i) May 5, 1987

At the NOAA-9 AVHRR overpass time (22:19:03 UT), the solar zenith angle (θ_s) was 38.5°. The nadir BRF data for May 5, 1987 were therefore interpolated at that sun angle, yielding the following reflectance factors:

	TM1	TM2	TM3	TM4	
Nadir BRF data (May 5, θ_s = 38.5°):	0.2521	0.3370	0.4014	0.4372	(1)

To adjust for any difference in surface reflectance between the pixel area and the BRF site, the nadir BRF data were interpolated at the average sun angle (30°) that prevailed during the pixel area measurements.

	TM1	TM2	TM3	TM4
Pixel area (May 5, θ_s = 30°):	0.2566	0.3361	0.3969	0.4272
BRF site (May 5, θ_s = 30°):	0.2594	0.3445	0.4105	0.4463
Ratio:	0.9892	0.9756	0.9669	0.9572

Thus, the adjusted reflectance factors are the earlier values (1) multiplied by the above ratio:

	TM1	TM2	TM3	TM4
Site-adjusted values:	0.2494	0.3288	0.3881	0.4185

These values were further corrected for the AVHRR view angle (θ_v) of -31.3° at the ground, where the negative sign indicates that the satellite was to the East of the site. BRF data acquired

at 22:22:00 (UT) for θ_s = 39° and θ_v = 30° were used. The AVHRR and BRF scan azimuth planes were within a few degrees of each other. The view angle correction factors, normalized with respect to nadir, are as follows:

	TM1	TM2	TM3	TM4
View angle factor (θ_v = -31.3°):	1.000	0.986	0.977	0.976

The final estimates of surface reflectance factor are the site-adjusted values multiplied by the view angle correction factor:

	TM1	TM2	TM3	TM4
Final values (May 5):	0.2494	0.3242	0.3792	0.4084

A reflectance value in MMR band 5 was estimated by applying the ratio between MMR bands 4 and 5, as measured by the MMR over the pixel area, to the final value just obtained for TM band 4:

MMR band 5 (pixel area, May 5):	0.4450
MMR band 4 (pixel area, May 5):	0.4272
Ratio:	1.0418
Final value TM band 4 (May 5):	0.4084
MMR band 5 final value (May 5):	0.4255

(ii) **May 4, 1987**

The approach for this date was similar to the one used for May 5, 1987, except that no ground measurements of surface reflectance were available. It was necessary to assume that the surface reflectance properties were not significantly different on the two days, a reasonable assumption given the nature of the surface (dry lakebed) and the clear weather conditions. At the NOAA-9 AVHRR overpass time (22:29:54 UT), the solar zenith angle was 40.7°. The nadir BRF data for May 5 and 6, 1987 were interpolated at that sun angle and averaged, yielding the following reflectance factors:

	TM1	TM2	TM3	TM4
Nadir BRF data (May 5 and 6, θ_s = 40.7°):	0.2506	0.3351	0.3989	0.4345

To adjust for any difference in surface reflectance between the pixel area and the BRF site, the nadir BRF data for May 5 and 6 were interpolated at the average sun angle (30°) that prevailed during the pixel area measurements on May 5 and 6, and then averaged.

	TM1	TM2	TM3	TM4
Pixel area (May 5, θ_s = 30°)	0.2566	0.3361	0.3969	0.4272
BRF site (May 5, θ_σ = 30°):	0.2594	0.3445	0.4105	0.4463
Ratio (May 5):	0.9892	0.9756	0.9669	0.9572
Pixel area (May 6, θ_s = 30°):	0.2503	0.3346	0.4002	0.4306
BRF site (May 6, θ_s = 30°):	0.2606	0.3459	0.4117	0.4472
Ratio (May 6):	0.9605	0.9673	0.9721	0.9629
Average ratio:	0.9748	0.9715	0.9695	0.9600

The adjusted reflectance factors are the initial values multiplied by the above average ratio:

	TM1	TM2	TM3	TM4
Site-adjusted values:	0.2443	0.3255	0.3867	0.4171

The AVHRR view angle was -15.3° at the ground and so BRF data acquired on May 5 at 22:22:00 (UT) for θ_s = 39° and θ_v = -15° were used to correct for view angle:

	TM1	TM2	TM3	TM4
View angle factor (θ_v = -15.3°)	0.986	0.982	0.977	0.980
Final values (May 4):	0.2409	0.3197	0.9778	0.4088

In this case, a reflectance value in MMR band 5 was obtained by applying the ratio between final values of TM band 4 and MMR band 5 on May 4 to the final value just obtained for TM band 4:

Final value, MMR band 5 (May 5):	0.4255
Final value, TM band 4 (May 5):	0.4084
Ratio:	1.0418
Final value TM band 4 (May 4):	0.4088
MMR band 5 final value (May 4):	0.4259

(iii) October 14, 1986

On this date, surface reflectance data were acquired over the pixel area site, but no BRF measurements were made. At the NOAA-9 AVHRR overpass time (21:46:55 UT), the solar zenith angle was 53.0°. The nadir data for May 6, 1987 were interpolated at the sun angle, yielding the

following reflectance factors:

	TM1	TM2	TM3	TM4
Nadir BRF data (May 6, θ_s = 53°):	0.2462	0.3286	0.3917	0.4265

The site adjustment was based on the average of the site adjustment factors for May 4 and May 5.

	TM1	TM2	TM3	TM4
May 4 site adjustment:	0.9892	0.9756	0.9669	0.9572
May 5 site adjustment:	0.9748	0.9715	0.9695	0.9600
Average:	0.9820	0.9736	0.9682	0.9586
Site-adjusted values:	0.2418	0.3199	0.3792	0.4088

The AVHRR view angle was +44.5° at the ground, where the positive sign indicates that the satellite was West of the site. There were no BRF data sets collected on any day with solar zenith angles as large as 53.0° in the afternoon. Instead, a roughly suitable configuration from a morning BRF data set was used, namely the BRF data acquired on May 5 at 16:13:04 (UT) for θ_s = 51.3° and θ_v = -44.5° (interpolated between -40° and -45°). A negative view angle was used for the BRF data because it is on the side of the sun (Eastward) in the morning, just as the satellite was on the side of the sun (Westward) in the afternoon. These BRF data would give rise to the following view angle factors:

	TM1	TM2	TM3	TM4
View angle factor (θ_v = -44.5°):	1.340	1.290	1.280	1.231

However, the relative azimuth between solar and sensor directions is not well matched to the BRF measurement configuration, being approximately 38° at the AVHRR observation and 2° for the relevant BRF data set. In order to compensate for this azimuth difference, the May and September BRF factors were compared, since the two time frames have different solar zenith/azimuth distributions. Comparing a May BRF data set with a small relative azimuth to a September BRF data set at the same solar zenith angle with a larger relative azimuth indicates that the view angle correction is reduced by close to a factor of two. The view angle correction that results is as follows:

	TM1	TM2	TM3	TM4
View angle factor (θ_v = -44.5°):	1.170	1.150	1.140	1.120
Final values (October 14):	0.2828	0.3679	0.4323	0.4579

The reflectance value in MMR band 5 was estimated by applying the ratio between MMR bands 4 and 5, as measured by the MMR over the pixel area, to the final value just obtained for TM band 4:

MMR band 5 (pixel area, Oct. 14):	0.4675
MMR band 4 (pixel, area, Oct. 14):	0.4446
Ratio:	1.0515
Final value TM band 4 (Oct. 14):	0.4579
MMR band 5 final value (Oct. 14):	0.4815